Journal of African Earth Sciences 66–67 (2012) 46–55

Contents lists available at SciVerse ScienceDirect

Journal of African Earth Sciences

journal homepage: www.elsevier.com/locate/jafrearsci

Geochemical evolution of groundwater in an alluvial aquifer: Case of El Eulma aquifer, East Algeria

Lazhar Belkhiri [a,*], Lotfi Mouni [b], Abderrahmane Boudoukha [c]

[a] University Hadj Lakhdar, 05000 Batna, Algeria
[b] Département des Sciences Techniques, Institut des Sciences, Université Akli Mohand Oulhadj, Bouira, Algeria
[c] Research Laboratory in Hydraulics Applied, University Hadj Lakhdar, 05000 Batna, Algeria

ARTICLE INFO

Article history:
Received 23 December 2010
Received in revised form 29 February 2012
Accepted 2 March 2012
Available online 12 March 2012

Keywords:
Groundwater
Cluster analysis
Geochemical modeling
PHREEQC
El Eulma Mio-Plio-Quaternary aquifer
Algeria

ABSTRACT

Hydrochemical, multivariate statistical and inverse hydrogeochemical modeling techniques were used to determine the main factors and mechanisms controlling the chemistry of groundwaters in the El Eulma Mio-Plio-Quaternary aquifer, East Algeria. Cluster analysis based on major ion contents defined three main chemical water types, reflecting different hydrochemical processes. The first, group 1, has low salinity (mean EC = 937 μS/cm) and abundance orders $Ca^{2+} > Na^{+} \approx Mg^{2+} > K^{+}$ and $HCO_3^{+} > Cl^{-} > SO_4^{2-} > NO_3^{-}$. With increased water–rock interaction, waters in groups 2 and 3 become more saline, changing composition towards Cl–HCO_3–Ca and Cl–Ca–Na types. The PHREEQC geochemical modeling demonstrated that relatively few phases are required to derive water chemistry in the area. In a broad sense, the reactions responsible for the hydrochemical evolution in the area fall into three categories: (1) dissolution of evaporite minerals; (2) precipitation of carbonate minerals, quartz, kaolinite and Ca-smectite; (3) ion exchange.

Published by Elsevier Ltd.

1. Introduction

The chemical composition of groundwater is controlled by many factors that include composition of precipitation, geological structure and mineralogy of the watersheds and aquifers, and geochemical processes within the aquifer. The interaction of all factors leads to various water facies. Usually, major ions studies are used to define hydrochemical facies of waters and the spatial variability can provide insight into aquifer heterogeneity and connectivity (Murray, 1996; Rosen and Jones, 1998). With the development of geochemical modeling, trace, major and isotopic elements are used to infer the physical and chemical processes controlling the water chemistry and to delineate flow paths in aquifer (Eberts and George, 2000; Plummer and Sprinckle, 2001; André, 2002; Güler and Thyne, 2004; Belkhiri et al., 2010).

In the literature, many different methodologies have been applied to study, evaluate and characterize the sources of variation in groundwater geochemistry. Among these methods are the multivariate techniques and inverse geochemical modeling. In recent years, multivariate statistical methods have been employed to extract critical information from hydrochemical datasets in complex systems. These techniques can help resolve hydrological factors such as aquifer boundaries, ground water flow paths, or hydrochemical components (Seyhan et al., 1985; Usunoff and Guzman-Guzman, 1989; Razack and Dazy, 1990; Join et al., 1997; Ochsenkuehn et al., 1997; Liedholz and Schafmeister, 1998; Suk and Lee, 1999; Wang et al., 2001; Locsey and Cox, 2003; Belkhiri et al., 2010), identify geochemical controls on composition (Adams et al., 2001; Alberto et al., 2001; Lopez-Chicano et al., 2001; Reeve et al., 1996), and separate anomalies such as anthropogenic impacts from the background (Hernandez et al., 1991; Birke and Rauch, 1993; Helena et al., 2000; Pereira et al., 2003) on a variety of scales (Briz-Kishore and Murali, 1992). Inverse geochemical modeling in PHREEQC (Parkhurst and Appelo, 1999) is based on a geochemical mole-balance model, which calculates the phase mole transfers (the moles of minerals and gases that must enter or leave a solution) to account for the differences in an initial and a final water composition along the flow path in a groundwater system. At least two chemical analyses of groundwater at different points of the flow path, and a set of phases (minerals and/or gases) which potentially react along this flow path are needed to populate the program (Charlton et al., 1997). A number of assumptions are inherent in the application of inverse geochemical modeling: (1) the two groundwater analyses from the initial and final waterwells should represent groundwater that flows along the same flow path, (2) dispersion and diffusion do not significantly affect groundwater chemistry, (3) a chemical steady-state prevails in the groundwater system during the time considered, and (4) the mineral phases used in the inverse calculation are or were present in the aquifer (Zhu and Anderson, 2002). The soundness or validity of the results in the inverse modeling depends on a valid

* Corresponding author.
E-mail address: BELKHIRI_Laz@yahoo.fr (L. Belkhiri).

1464-343X/$ - see front matter Published by Elsevier Ltd.
http://dx.doi.org/10.1016/j.jafrearsci.2012.03.001

conceptualization of the groundwater system, validity of the basic hydrochemical concepts and principles, accuracy of input data into the model, and level of understanding of the geochemical processes in the area (Güler and Thyne, 2004).

This study tries to answer mainly these questions. The main objectives of this paper are: (1) to assess the chemistry of groundwater and (2) to identify geologic factors that presently affect the water chemistry in the region by using multivariable statistical and geochemical modeling techniques.

2. Geology and hydrogeology

The area of study is located in the East of Algeria (Fig. 1). The climate of the study area is considered to be semi-arid, the annual precipitation being approximately 421 mm. The rainy season extends from October to May, with a maximum during December and March off each year. The mean monthly temperatures varying between −3 and 38 °C, the mean annual value being 15 °C. The vegetation of the study area is characterized by grasses and herbs. Soils are generally sandy to clayey in texture and mostly classified as Aridisol and are calcareous. Mineralogically, most of the soils are dominated by kaolinite, illite, smectite, and chlorite, typical for most arid and semi-arid soils. The presence of smectite suggests specific sites for sodium adsorption. Most of its inhabitants are concentrated in the town of El Eulma with more than 30,000 inhabitants working mainly in the production of cereals (barley, corn).

Rocks and unconsolidated deposits in the area can be divided into three geologic units (Savornin, 1920; Galcon, 1967; Guiraud, 1973; Vila, 1980): (1) upper Cretaceous (Senonian); (2) Eocene; (3) Mio-Plio-Quaternary. Senonian (upper Cretaceous) is generally found in the northern part of the study area. Senonian units are composed of Santonian–Campanian formation and upper Senonian formation. These formations are consists various rocks with differing compositions including limestone and marl of about 550 m thick. Eocene units are composed of Ypresian–Lutetian formation (Fig. 1). Eocene rocks consist of a succession of marine, limestone and silt of about 80 m thick. The Mio-Plio-Quaternary is a heterogeneous continental detrital sedimentation.

The studied area is situated in the alluvial plain of the Mio-Plio-Quaternary. Shallow groundwater mainly occurs 5–80 m below the surface. Groundwater is recharged by vertically infiltrating meteoric water in the basin and by stream water coming from different reliefs surrounding the depression inter-mountainous of El Eulma. Evapotranspiration and artificial abstraction are the major processes of shallow groundwater discharge. The direction of groundwater flow around El Eulma plain is from south to NE–SW in east and north, NW–SE in west. In general, the groundwater flows toward the center of the plain (Fig. 2). The pumping tests on different wells showed high transmissivity (10^{-3} m^2/s) indicating high yields.

3. Materials and methods

3.1. Sample collection and analysis

A set of 38 groundwater samples was analyzed for 11 physical and chemical parameters comprising major ion concentrations (Ca^{2+}, Mg^{2+}, Na^{+}, K^{+}, Cl^{-}, SO_4^{2-}, HCO_3^{-}, NO_3^{-}), electrical conductivity (EC), pH and the temperature (*T*). The samples were taken from wells located in the El Eulma aquifer, East Algeria (Fig. 1). The samples were collected after pumping for 10 min. This was done to remove groundwater stored in the well. These samples were collected using 4–1 acid-washed polypropylene containers. Each sample was immediately filtered on site through 0.45 μm filters on acetate cellulose. Filtrate for metals analyses were transferred into 100-cm^3 polyethylene bottles and immediately acidified to pH < 2 by the addition of Merck™ ultrapure nitric acid (5 ml 6 N HNO_3). Samples for anions analyses were collected into 250-cm^3 polyethylene bottles without preservation. All the samples were stored in an ice chest at a temperature of <4 °C and later

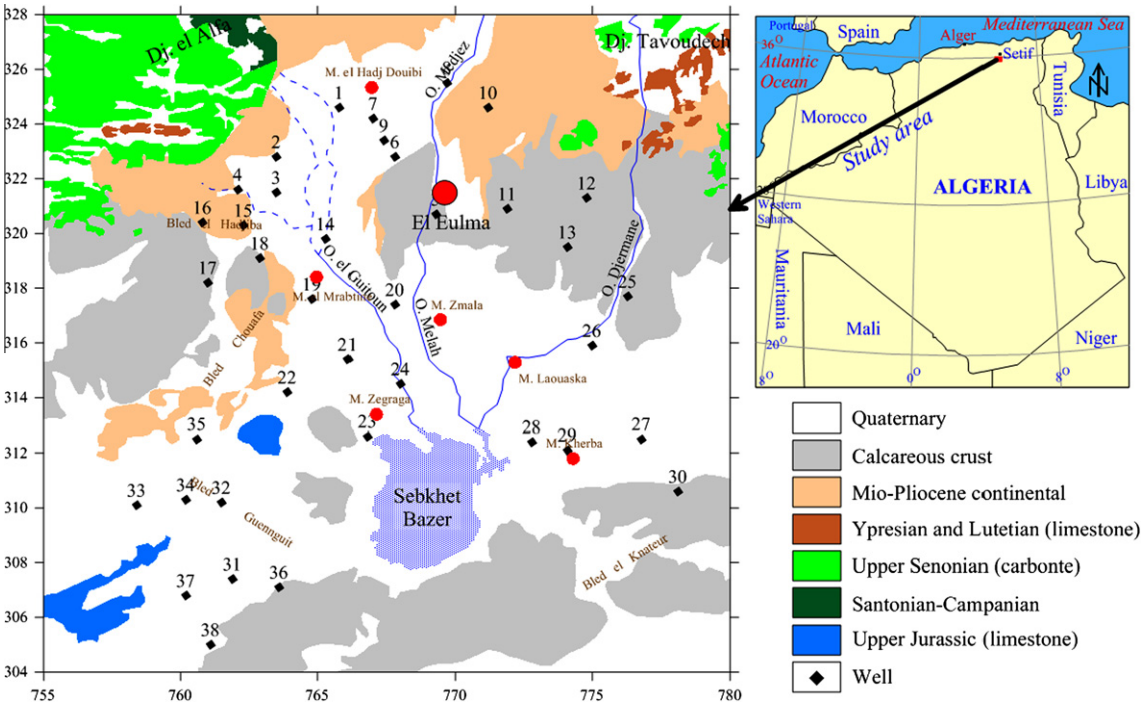

Fig. 1. Location map of the study area showing the sampling locations.

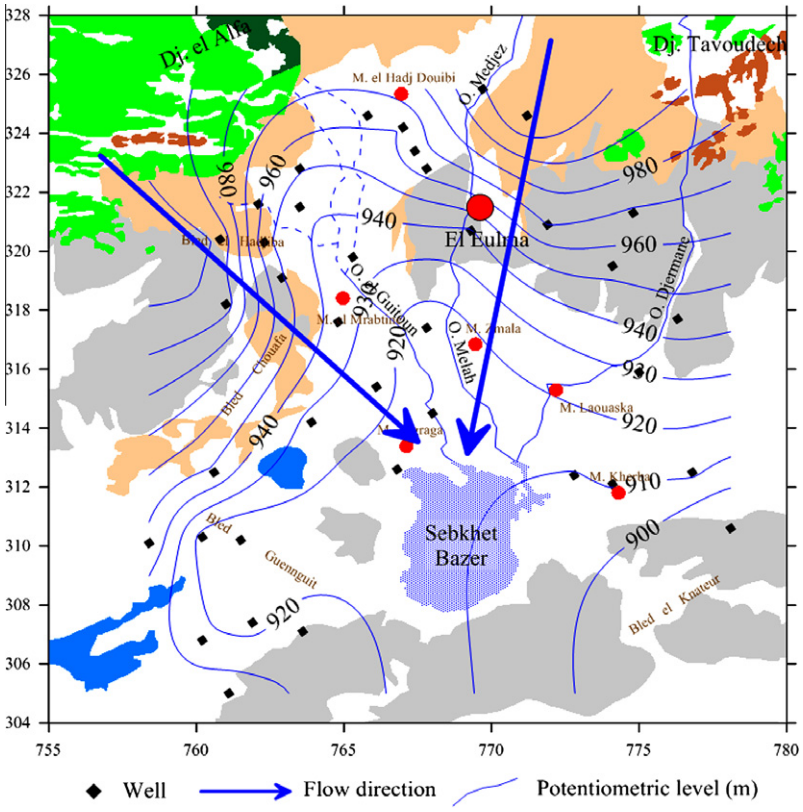

Fig. 2. Potentiometric surface of the El Eulma aquifer.

transferred to the laboratory and stored in a refrigerator at a temperature of <4 °C until analyzed (within 1 week). Immediately after sampling, temperature, pH and electrical conductivity (EC) were measured in the field using a multi-parameter WTW (P3 MultiLine pH/LF-SET). Subsequently, the samples were analyzed in the laboratory for their chemical constituents such as calcium, magnesium, sodium, potassium, chloride, bicarbonate, sulfate, and nitrate. This was achieved using standard methods as suggested by the American Public Health Association (APHA, 1989, 1995a,b). Ca^{2+}, Mg^{2+}, HCO_3^- and Cl^- were analyzed by volumetric titrations. Concentrations of Ca^{2+} and Mg^{2+} were estimated titrimetrically using 0.05 N EDTA and 0.01 N and those of HCO_3^- and Cl^- by H_2SO_4 and $AgNO_3$ titration, respectively. Concentrations of Na^+ and K^+ were measured using a flame photometer (Model: Systronics Flame Photometer 128) and that of sulfate (SO_4^{2-}) by turbidimetric method (Clesceri et al., 1998). Nitrate (NO_3^-) was analyzed by colorimetry with a UV–visible spectrophotometer (Rowell, 1994). Standard solutions for the above analysis were prepared from the respective salts of analytical reagents grades. The accuracy of the chemical analysis was verified by calculating ion-balance errors where the errors were generally within 10%.

3.2. Cluster analysis

Cluster analysis refers to a set techniques designed to classify observations so members of the resulting groups are similar to each other but distinct from other groups. Hierarchical clustering, which successively joins the most similar observations, is the most common approach (Davis, 1986). While other multivariate techniques, such as factor analysis or principal component analysis, provide more insight into the underlying structure of a data set, the use of these techniques might require further analyses to identify distinct groups. Cluster analysis on the other hand, may be thought of as a useful way of objectively organizing a large data-set into groups on the basis of a given set of characteristics. This can ultimately assist in the recognition of potentially meaningful patterns (Swanson et al., 2001). Hydrochemical results of all samples were statistically analyzed by using the software STATISTICA® (1998).

3.3. Inverse geochemical modeling

Inverse modeling calculations were performed using PHREEQC (Parkhurst and Appelo, 1999). PHREEQC was also used to calculate

Table 1
Chemical summary of shallow groundwater in the study area.

	EC	T	pH	Ca^{2+}	Mg^{2+}	Na^+	K^+	Cl^-	SO_4^{2-}	HCO_3^-	NO_3^-
WHO	750	25	7–8.5	75	30	50	100	250	250	300	50
Min	608	7.9	7.8	60.12	10.09	25.29	1.56	49.63	36.02	122	8.68
Max	3577	14.9	8.5	288.6	74.13	451.7	9.38	753.7	278.6	366.1	161.2
Mean	1431	11.16	8.13	141.71	33.1	105.69	4.54	219.65	152.98	228.32	73.59
SD	620	2.04	0.19	53.99	17.51	90.47	2.1	164.53	59.17	62.13	37.67
Cv	43	18.29	2.38	38.1	52.91	85.6	46.36	74.91	38.68	27.21	51.19

All values are in mg/l except pH, *T* (°C) and EC (μ.Siemens/cm). WHO (2006).

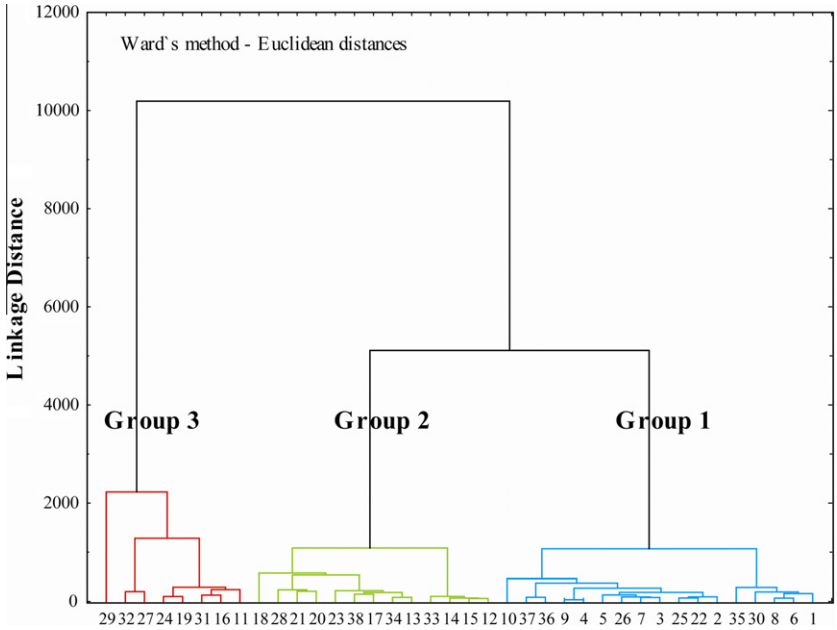

Fig. 3. Q-mode cluster analysis. Dendrogram for 38 samples and seven chemical variables.

Table 2
Parameter values of the three principal water groups.

	Group 1					Group 2					Group 3				
	Min	Max	Mean	SD	Cv	Min	Max	Mean	SD	Cv	Min	Max	Mean	SD	Cv
EC	608	1072	937	132	14	1255	1764	1479	164	11	2016	3577	2403	518	22
T	8.50	14.90	11.36	2.26	19.88	7.90	13.70	11.05	1.94	17.54	8.30	13.50	10.93	1.94	17.72
pH	7.90	8.50	8.17	0.19	2.32	7.80	8.40	8.18	0.17	2.07	7.80	8.30	7.99	0.19	2.36
Ca^{2+}	60.12	270.5	119.56	48.76	40.78	76.15	236.5	138.74	42.57	30.69	130.3	288.6	193.58	50.84	26.27
Mg^{2+}	12.15	58.70	25.06	12.36	49.34	10.09	70.85	37.09	17.20	46.38	17.01	74.13	43.69	21.20	48.52
Na^{+}	25.29	99.78	53.21	18.61	34.97	59.77	232.20	106.80	56.06	52.49	105.80	451.70	215.40	128.99	59.89
K^{+}	1.56	9.38	3.98	1.98	49.65	1.56	9.38	4.30	2.25	52.22	3.91	7.82	6.11	1.46	23.93
Cl^{-}	49.63	308.4	111.75	58.62	52.46	99.27	555.9	233.51	109.95	47.08	265.9	753.70	426.41	192.42	45.13
SO_4^{2-}	36.02	240.1	134.1	51.4	38.33	52.83	273.80	140.63	57.85	41.14	163.3	278.6	213.19	37.94	17.79
HCO_3^{-}	122	366.1	244.37	67.67	27.69	122	280.7	202.3	48.64	24.04	183.1	335.6	236.48	62.61	26.48
NO_3^{-}	8.68	161.2	60.03	35.57	59.26	43.4	151.9	89.52	35.37	39.51	32.86	155	76.50	39.18	51.22

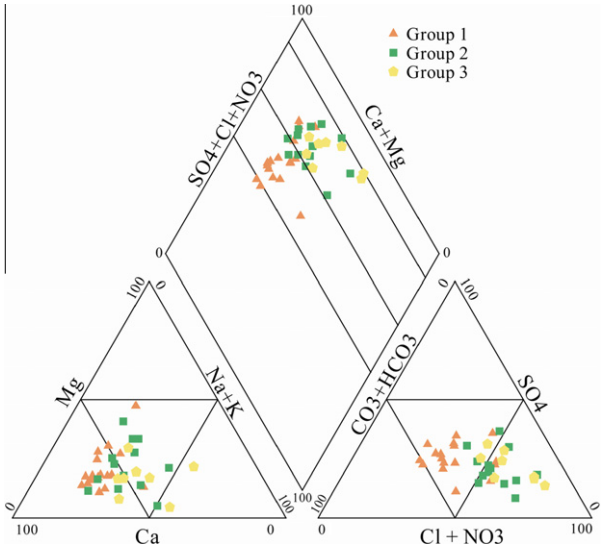

Fig. 4. Piper diagram for water samples.

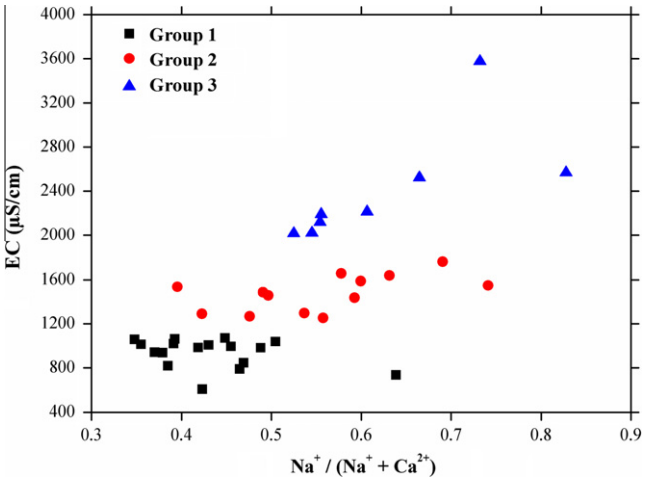

Fig. 5. $[Na^+/(Na^+ + Ca^{2+})]$ vs. EC plot.

aqueous speciation and mineral saturation indices. Inverse modeling in PHREEQC uses the mass-balance approach to calculate all the stoichiometrically available reactions that can produce the observed chemical changes between end-member waters (Plummer and Back, 1980). This mass balance technique has been used to quantify reactions controlling water chemistry along flow paths (Thomas et al., 1989) and quantify mixing of end-member components in a flow system (Kuells et al., 2000). Minerals used in the inverse geochemical models are limited to those present in the study area (Belkhiri et al., 2010).

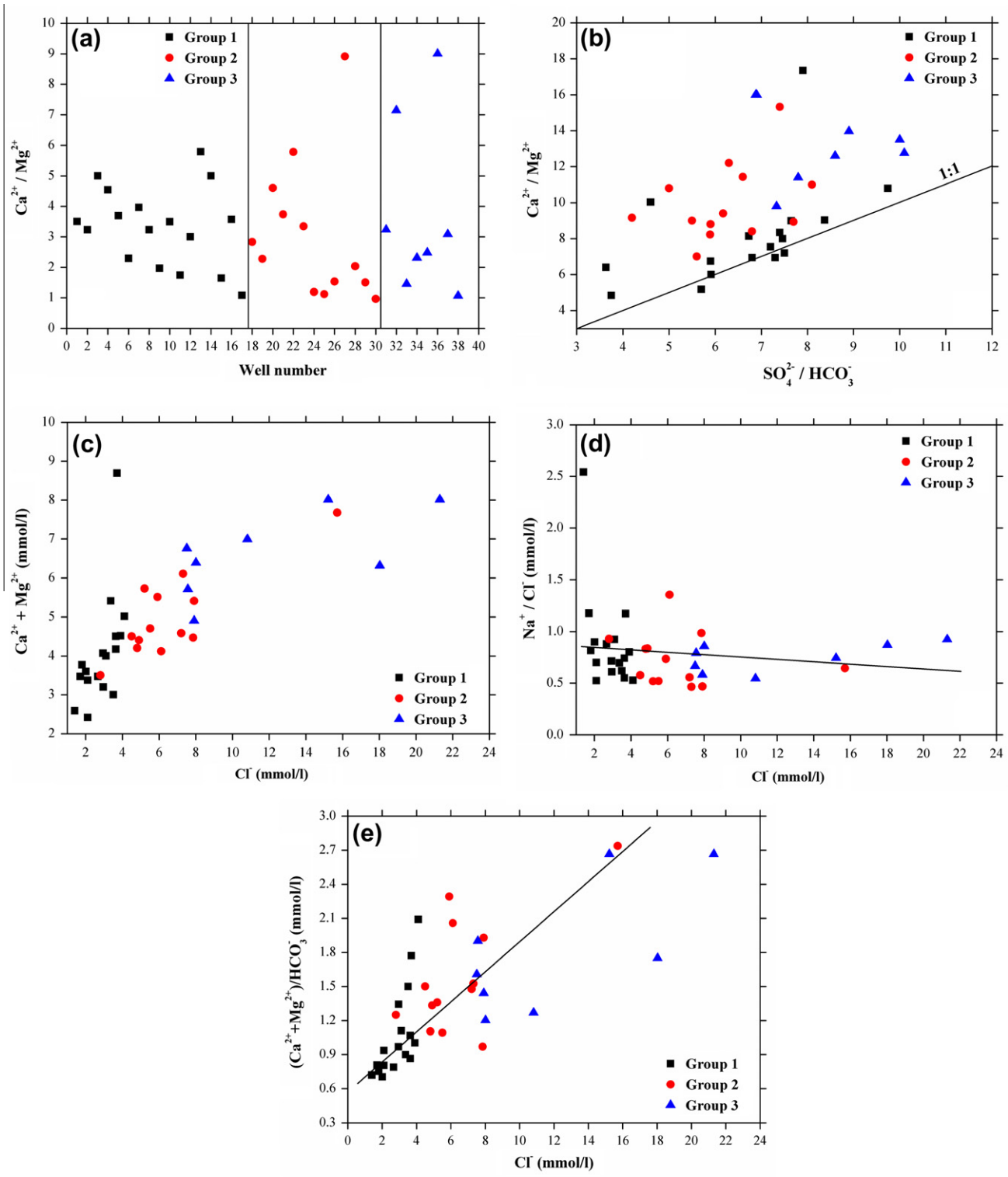

Fig. 6. Relationships well number vs. Ca^{2+}/Mg^{2+} (a), $Ca^{2+} + Mg^{2+}$ vs. $SO_4^{2-} + HCO_3^-$ (b), $Ca^{2+} + Mg^{2+}$ vs. Cl^- (c), Na^+/Cl^- vs. Cl^- (d) and $[(Ca^{2+} + Mg^{2+})/HCO_3^-]$ vs. Cl^- (e) for waters from the study area.

4. Results and discussion

4.1. General hydrochemistry

Table 1 presents the statistical summary of all the parameters analyzed. The mean concentrations of the major ions in the Quaternary aquifer are within the WHO (2006) guidelines for drinking water. The electrical conductivity of groundwater samples ranges from 608 to 3577 μS/cm with a mean value of 1431 μS/cm. The salinity increases in the direction of groundwater flow from north to south. The pH ranges between 7.8 and 8.5 with a mean value of 8.13 (Table 1). The mean temperature of waters was 11.16 °C. This shows that the groundwater of the study area is mainly of alkaline in nature. Cl^- and HCO_3^- are the major anions and Ca^{2+} and Mg^{2+} are the major cations in shallow groundwater in El Eulma plain. The relative abundance of the ions is $Ca^{2+} > Na^{2+} > Mg^{2+} > K^+$ (on molar basis) and $Cl^- > HCO_3^- > SO_4^{2-} > NO_3^-$ (Table 1). The maximum Ca^{2+} and Mg^{2+} concentrations of 288.6 mg/l and 74.13 mg/l respectively are, however, higher than their respective WHO (2006) standards of 75 mg/l and 30 mg/l. The prevailing common lithology is carbonate rocks mainly the limestone and dolomite, widely in the study area. The common source of calcium and magnesium in the groundwater is limestone and dolomite in the sedimentary rocks. The mean sodium and potassium concentrations in the groundwater are 105.69 mg/l and 4.54 mg/l, respectively. The presence of bicarbonate ions HCO_3^- in the groundwater is derived from carbon dioxide in the atmosphere, soils and by dissolution of carbonate rocks. Bicarbonate ion represents the second dominance anion in the study area. The concentration in most of northern part of the study reaches about 366.1 mg/l. The chloride ion is widely distributed in natural water. Most Cl^- in the groundwater is from three sources including ancient seawater entrapped in sediment, solution of halite and related minerals in evaporate deposits in the region. The value of the chloride in the study area ranges between 49.63 and 753.7 mg/l. The most extensive and important occurrences of sulfate ions in the investigated water are sedimentary rocks such as gypsum ($CaSO_4{\cdot}2H_2O$) and anhydrite ($CaSO_4$). During weathering, the sulfides, which are in contact with water, are oxidized to yield sulfate that is carried off in water. In the study area, the leaching of sulfate from the upper soils causes the sulfate to be the principle anion in the groundwater. Further addition of sulfate to the groundwater comes from the breakdown of organic matters in the soil, and from addition of leachable sulfates in fertilizers of the intensively cultivated areas in El Eulma plain. The value of SO_4^{2-} in the study area ranges between 36.02 and 278.6 mg/l. Almost 42% of the samples exceeded the desirable limit of Cl^- (250 mg/l), but only 18.4% of them exceed that of SO_4^{2-} (250 mg/l) (WHO, 2006). Most samples exceeded the desirable limit of NO_3^- for drinking water (50 mg/l) (WHO, 2006). In the study area, samples with high NO_3^- values were mainly taken near urban areas. The high concentration of NO_3^- is likely to be related to wastewater leakage from industrial activities, urbanization and agricultural practices. NO_3^- concentration is also high in areas of intensive agriculture, reaching a maximum of 161.2 mg/l.

4.2. Hydrochemical water types

To identify possible groups of waters based on major chemical compositions, ion species Ca^{2+}, Mg^{2+}, Na^+, K^+, Cl^-, SO_4^{2-}, HCO_3^- and NO_3^- were con considered for application of a clustering Q-technique, in which similarity relationships among water samples were examined. The clustering procedure was performed by the Ward's linkage method with the Euclidean distance as a measure of similarity of samples. Results are displayed in the dendrogram of Fig. 3, which shows that, three preliminary groups are selected based on visual examination of the dendogram, each representing a hydrochemical facies with means for each parameter shown in Table 2. From a geochemical viewpoint, these groups are interpreted by plotting the representative points of water samples on Piper diagram (Piper, 1994) (Fig. 4) and the $[Na^+/(Na^+ + Ca^{2+})]$ – EC plot (Fig. 5).

The first group of waters, group 1, has low salinity (mean EC = 937 μS/cm) and abundance orders (meq/l) $Ca^{2+} > Na^+ \approx Mg^{2+} > K^+$ and $HCO_3^- > Cl^- > SO_4^{2-} > NO_3^-$ (Fig. 4). These waters are classified as HCO_3^--alkaline earth water type. Most of the HCO_3^-, whose mean concentration is 244.37 mg/l, is probably derived from carbonate precipitation.

Group 2 is made up of water samples the cation composition of which is dominated by Ca^{2+} and Na^{2+}, with anion composition varying from dominantly Cl^- to dominantly HCO_3^- plus SO_4^{2-} (Fig. 4). EC (mean 1479 μS/cm) are significantly greater than those of group 1, reflecting a more effective weathering process (Fig. 5).

Group 3, made up of eight water samples, has a salinity range (2016 < EC < 3577 μS/cm; mean 2403 μS/cm) overlapping that of the previous group. On the basis of overall chemical composition, characterized by ion abundances $Ca^{2+} \approx Na^+ > Mg^{2+} > K^+$ and $Cl^- > SO_4^{2-} > HCO_3^- > NO_3^-$, these waters are classified as Cl^-–

Table 3
Statistical summary of thermodynamic speciation calculations using PHREEQC.

	Anhydrite	Aragonite	Calcite	$CO_{2(g)}$	Dolomite	Gypsum	Halite
Group 1							
Min	−2.33	0.45	0.60	−3.47	0.59	−2.08	−7.26
Max	−1.35	0.84	0.99	−2.45	1.81	−1.09	−6.47
Mean	−1.65	0.68	0.84	−2.92	1.13	−1.40	−6.88
SD	0.24	0.13	0.13	0.30	0.31	0.24	0.23
Cv	−14.72	19.29	15.80	−10.24	27.63	−17.39	−3.36
Group 2							
Min	−2.05	0.31	0.46	−3.30	−0.09	−1.80	−6.79
Max	−1.26	0.95	1.10	−2.70	1.79	−1.01	−5.50
Mean	−1.61	0.64	0.80	−3.02	1.14	−1.35	−6.26
SD	0.20	0.18	0.18	0.17	0.48	0.20	0.33
Cv	−12.59	27.65	22.33	−5.71	42.50	−14.99	−5.33
Group 3							
Min	−1.47	0.20	0.36	−2.93	0.32	−1.22	−6.11
Max	−1.23	1.08	1.24	−2.61	2.08	−0.98	−5.09
Mean	−1.34	0.62	0.77	−2.77	1.00	−1.09	−5.73
SD	0.08	0.29	0.29	0.11	0.66	0.08	0.41
Cv	−5.88	46.60	37.21	−4.08	65.43	−7.11	−7.11

Ca^{2+}–Na^{+} type (Fig. 4). The most pronounced characteristic in this group is the increase in the Cl^{-} content.

4.3. Ionic relations and sources of major components in the groundwater

The rock dominance of the major-ion chemistry in the region provides an insight of chemical weathering in the aquifer, since weathering of different parent rocks (e.g., carbonates, silicates, and evaporites) yields different combinations of dissolved cations and anions to solution. For example, Ca^{2+} and Mg^{2+} originate from the weathering of carbonates, silicates and evaporites, Na^{+} and K^{+} from the weathering of evaporites and silicates, HCO_3^{-} from carbonates and silicates, SO_4^{2-} and Cl^{-} from evaporites, while silica exclusively sources from the weathering of silicates (Chen, 1987).

The study of the Ca^{2+}/Mg^{2+} ratio of groundwater from this area also supports the dissolution of calcite and dolomite present in the aquifer (Fig. 6a). That is, if the ratio $Ca^{2+}/Mg^{2+} = 1$, dissolution of dolomite should occur, whereas a higher ratio is indicative of greater calcite contribution (Maya and Loucks, 1995). Higher Ca^{2+}/Mg^{2+} molar ratio (>2) indicates the dissolution of silicate minerals, which contribute calcium and magnesium to groundwater (Katz et al., 1998). In Fig. 6a, the points closer to the line ($Ca^{2+}/Mg^{2+} = 1$) indicate the dissolution of dolomite. All of the samples having a ratio greater than 1 indicate the dissolution of calcite. Those with values greater than 2 indicate the effect of silicate minerals (Fig. 6a).

The plot of $Ca^{2+} + Mg^{2+}$ vs. $SO_4^{2-} + HCO_3^{-}$ will be close to the 1:1 line if the dissolutions of calcite, dolomite and gypsum are the dominant reactions in a system. Ion exchange tends to shift the points to the right due to an excess of $SO_4^{2-} + HCO_3^{-}$ (Cerling et al., 1989; Fisher and Mulican, 1997). If reverse ion exchange is the process, it will shift the points to the left due to a large excess of $Ca^{2+} + Mg^{2+}$ over $SO_4^{2-} + HCO_3^{-}$, which can be explained by the following reaction:

$$2Na^{+} + Ca(Mg)clay \leftrightarrow Na - clay + Ca^{2+}(Mg^{2+}) \quad (1)$$

The plot of $Ca^{2+} + Mg^{2+}$ vs. $SO_4^{2-} + HCO_3^{-}$ (Fig. 6b) shows that the samples of the second and the last groups are distributed on both sides but reverse ion exchange tends to dominate over ion exchange. On the other hand, most the points of the group 1 are clustered around and above the 1:1 line. An excess of calcium and magnesium in the groundwater of Mio-Plio-Quaternary aquifer may be due to the exchange of sodium in the water by calcium and magnesium in clay material.

The plot of $Ca^{2+} + Mg^{2+}$ vs. Cl^{-} (Fig. 6c) indicates that Ca^{2+} and Mg^{2+} increase with increasing salinity. The plots of Na^{+}/Cl^{-} vs. Cl^{-} (Fig. 6d) and $Ca^{2+} + Mg^{2+}$ vs. Cl^{-} (Fig. 6c) clearly indicate that salinity increases with the decrease in Na^{+}/Cl^{-} and increase in $Ca^{2+} + Mg^{2+}$, which may be due to reverse ion exchange in the clay/weathered layer. During this process, the aquifer matrix may adsorb dissolved sodium in exchange for bound Ca^{2+} and Mg^{2+}. The sources of Ca^{2+} and Mg^{2+} in groundwater can be deduced from the $(Ca^{2+} + Mg^{2+})/HCO_3^{-}$ ratio. As this ratio increases with salinity (Fig. 6e), Mg^{2+} and Ca^{2+} are added to solution at a greater rate than HCO_3^{-}.

In natural systems, carbonate minerals dissolution can be written as (Garrels and Mackenzie, 1971):

$$CaCO_3(Calcite) + H_2CO_3 \rightarrow Ca^{2+} + 2HCO_3^{-} \quad (2)$$

$$CaMg(CO_3)_2(dolomite) + H_2CO_3 \rightarrow Ca^{2+} + Mg^{2+} + 4HCO_3^{-} \quad (3)$$

$$CaCO_3 + H_2SO_4 \rightarrow Ca^{2+} + SO_4^{-} + H_2CO_3 \quad (4)$$

$$CaMg(CO_3)_2 + 2H_2SO_4 \rightarrow Ca^{2+} + Mg^{2+} + 2SO_4^{-} + 2H_2CO_3 \quad (5)$$

4.4. Mineral stability diagrams

In order to investigate thermodynamic controls on the water composition, equilibrium speciation calculation was made using PHREEQC (Parkhurst and Appelo, 1999). These calculations provided saturation indices (SIs) of minerals that might be reacting in the system. The SI of a particular mineral can be defined as

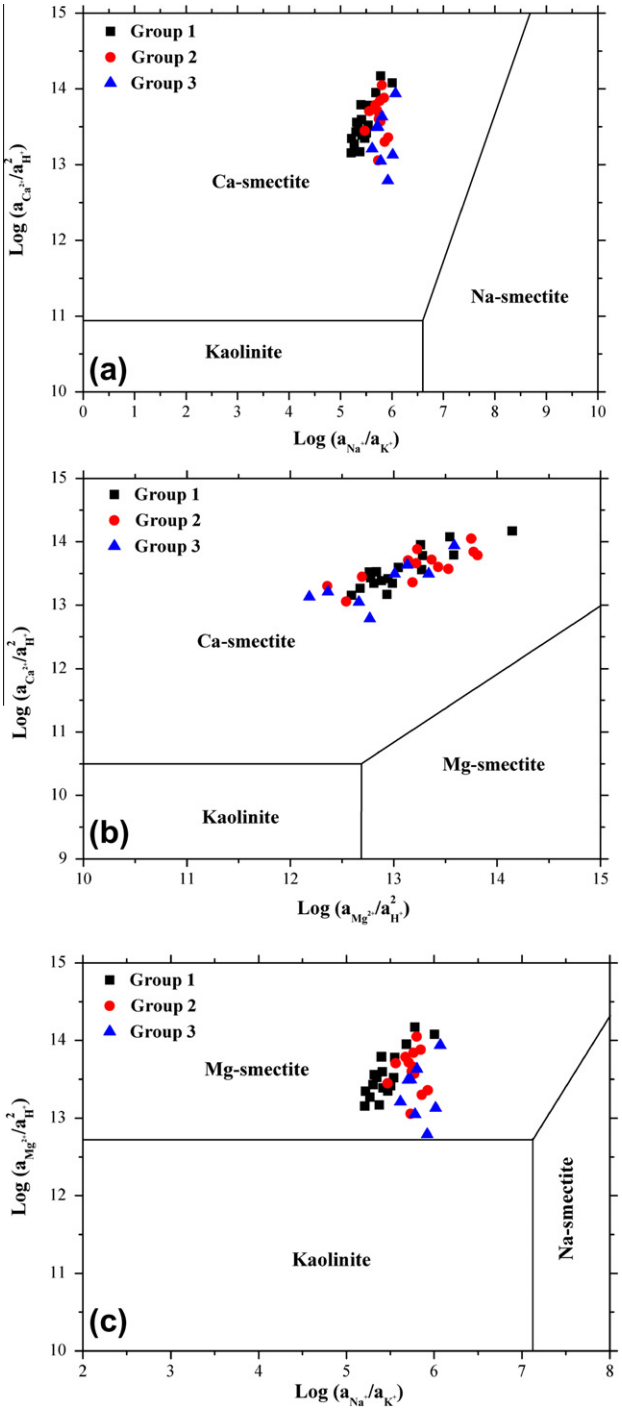

Fig. 7. Selected activity diagrams in $CaO–Na_2O–Al_2O_3–SiO_2–H_2O$, $CaO–MgO–Al_2O_3–SiO_2–H_2O$ and $MgO–Na_2O–Al_2O_3–SiO_2–H_2O$ systems at 25 °C and 1 bar. Activity plots of **(a)** $\log(a_{Ca}/a_H^2)$ vs. $\log(a_{Na}/a_H)$, **(b)** $\log(a_{Ca}/a_H^2)$ vs. $\log(a_{Mg}/a_H^2)$ and **(c)** $\log(a_{Mg}/a_H^2)$ vs. $\log(a_{Na}/a_H)$.

$$SI = \log(IAP/K) \quad (6)$$

where IAP denotes the Ion Activity Product and K refers to the equilibrium constant. Equilibrium is indicated when SI = 0. If SI > 0, then the groundwater is super-saturated (i.e., precipitation is required to achieve equilibrium), and if SI < 0, then the groundwater is under-saturated (dissolution is required to achieve equilibrium). The SI values of the water samples were listed in Table 3.

The results of saturation calculations show that all groups are super-saturated with respect to aragonite, calcite and dolomite (carbonate minerals). Anhydrite, gypsum and halite (evaporate minerals) are under-saturated in all groups suggesting that their soluble component Na^+, Cl^-, Ca^{2+} and SO_4^{2-} concentrations are not limited by mineral equilibrium.

Another approach to test the proposed hydrochemical evolution is the use of mineral stability diagrams (Drever, 1988). Fig. 7 shows four mineral stability diagrams for the $CaO–Na_2O–Al_2O_3–SiO_2–H_2O$ system (Fig. 7a), $CaO–MgO–Al_2O_3–SiO_2–H_2O$ system (Fig. 7b) and the $MgO–Na_2O–Al_2O_3–SiO_2–H_2O$ system (Fig. 7c). The values from 38 samples representing each of the three principle water groups are plotted on the diagrams to help define the reactions that control the water chemistry. In these diagrams (Fig. 7a–c) the waters plot essentially in the kaolinite stability field, indicating that equilibrium with this mineral phase is one of the main processes controlling water chemistry. It should also be noted that in Fig. 7b and c some samples extend into the Ca-smectite and Mg-smectite stability field. Therefore, the study of all of these stability diagrams prepared using the activity of ions revealed that the following are the major geochemical reactions controlling the groundwater chemistry of this region:

$$6CaAl_2SiO_{10}(OH)_2(Ca-\text{smectite}) + 2H^+ + 23H_2O \leftrightarrow 7Al_2Si_2O_5(OH)_4(\text{Kaolinite}) + Ca^{2+} + 8H_4SiO_4a^2 + 8H_4SiO_4 \quad (7)$$

$$MgAl_2SiO_{10}(OH)_2(Mg-\text{smectite}) + 2H^+ + 23H_2O \leftrightarrow 7Al_2Si_2O_5(OH)_4(\text{Kaolinite}) + Mg^{2+} + 8H_4SiO_4 \quad (8)$$

4.5. Inverse geochemical modeling

Potential phases in the inverse modeling were constrained (precipitation/dissolution) using compiled data of saturation indices derived from PHREEQC and a conceptual model inferred from general trends in chemical analyses data of groundwater. The inverse model was constrained so that primary mineral phases including gypsum, anhydrite, halite and carbon dioxide (gas) were set to dissolve until they reached saturation, and calcite, aragonite, kaolinite, quartz and Ca-smectite were set to precipitate once they reached saturation. Cation exchange reactions of Ca^{2+} for Na^+ on exchange sites were included in the model as a source for excess Na^+ in groundwater. The models in Table 3 were selected from all the possible models based on the statistical measurements calculated by PHREEQC (sum of residuals and maximum fractional error) and to represent different possible combinations of reactants and products that can account for the change in water chemistry. An inverse model describing the evolution of group 1 to group 2 waters (Model 1) and group 2 to group 3 waters (Model 2) can be written as (Table 4):

Model 1: Group 1 waters + dolomite + anhydrite + gypsum + halite + Ca-smectite + Ca from ion exchange + CO_2 gas → Group 2 waters + aragonite + calcite + kaolinite + quartz + Na loss to ion exchange.

Model 2: Group 2 waters + anhydrite + gypsum + halite + Ca from ion exchange + CO_2 gas → Group 3 waters + aragonite + calcite + dolomite + kaolinite + quartz + Ca-smectite + Na loss to ion exchange.

In geochemical modeling, results are dependent upon valid conceptualization of the system, validity of basic concepts and principles, accuracy of input data, and level of understanding of the geochemical processes (Güler and Thyne, 2004). The mass-balance modeling has shown that relatively few phases are required to derive observed changes in water chemistry and to account for the hydrochemical evolution in the El Eulma plain. In a broad sense, the reactions responsible for the hydrochemical evolution in the area fall into three categories: (1) dissolution of evaporite minerals; (2) precipitation of carbonate minerals, quartz, kaolinite and

Table 4
Results of inverse modeling using the means of each statistical group as input.

Mineral phases	Phase mol transfers Group 1–Group 2					
Aragonite	–	–	−1.37E−03	–	−1.37E−03	−8.44E−01
Calcite	−1.37E−03	−1.37E−03	−9.81E−04	−8.44E−01	−9.81E−04	−9.81E−04
Dolomite	3.89E−04	3.89E−04	–	2.62E−04	–	4.96E−04
Anhydrite	–	1.71E−04	–	–	1.71E−04	–
Gypsum	1.71E−04	–	1.71E−04	–	–	–
Halite	3.81E−03	3.81E−03	3.81E−03	3.41E−03	3.81E−03	3.41E−03
$CO_{2(g)}$	–	–	–	8.42E−01	–	8.42E−01
Kaolinite	−2.13E−03	−2.13E−03	−2.13E−03	−5.95E+00	−2.13E−03	−5.95E+00
Quartz	−2.45E−03	−2.45E−03	−2.45E−03	−6.84E+00	−2.45E−03	−6.84E+00
Ca-smectite	1.83E−03	1.83E−03	1.83E−03	5.11E+00	1.83E−03	5.11E+00
Ca-ion exchange	8.98E−04	8.98E−04	8.98E−04	8.41E−04	8.98E−04	8.41E−04
Na-ion exchange	−1.80E−03	−1.80E−03	−1.80E−03	−1.68E−03	−1.80E−03	−1.68E−03
	Phase mol transfers Group 2–Group 3					
Aragonite	–	−2.89E−04	−2.89E−04	–	−2.89E−04	−1.33E−04
Calcite	−9.66E−05	–	−2.89E−04	–	–	−2.89E−04
Dolomite	−3.30E−04	–	–	−3.32E−04	−3.32E−04	−3.32E−04
Anhydrite	–	7.40E−04	–	–	7.85E−04	4.80E−04
Gypsum	7.88E−04			7.81E−04	5.67E−03	5.67E−03
Halite	5.71E−03	2.57E−03	5.67E−03	5.67E−03	–	4.32E−03
$CO_{2(g)}$	2.36E−05	–	2.36E−05	3.12E−04	–	3.12E−04
Kaolinite	1.97E−03	−2.17E+01	–	−2.07E+01	−2.07E+01	–
Quartz	–	−2.50E+01	–	−2.38E+01	−2.38E+01	–
Ca-smectite	–	−1.75E−03	−1.69E−03	–	−1.77E−03	–
Ca-ion exchange	6.09E−04	–	5.70E−04	–	5.70E−04	3.11E−04
Na-ion exchange	−1.22E−03	–	−1.14E−03	–	−1.14E−03	−6.23E−04

Thermodynamic database used: phreeqc.dat values are in mol/kg H_2O. Positive (mass entering water) and negative (mass leaving water) phase mole transfers indicate dissolution and precipitation, respectively. – No mass transfer.

Ca-smectite; (3) ion exchange. The mineral phases were selected based on geologic descriptions and analysis of rocks and sediments from the area.

In the recharge area (group 1), the dominant geochemical process is the dissolution of carbonate and evaporite minerals, which contributes the Ca^{2+}, Mg^{2+}, and HCO_3^- to the groundwater. Chemical analysis of groundwater shows a general increase of Ca^{2+}, Mg^{2+}, EC and pH as the groundwater moves away from the recharge area (down gradient) which could be the result of carbonate (dolomite) and evaporite (gypsum) minerals dissolution (Model 1). Localized gypsum dissolution along the flow path contributes both Ca^{2+} and SO_4^{2-} to groundwater. The Ca^{2+} released by the dissolution of gypsum leads to the precipitation of additional calcite and an increase in CO_2, which leads to a slightly low pH and super-saturation or near equilibrium of groundwater with calcite. This phenomenon is referred to as common-ion driven precipitation or common ion effect (Back and Hanshaw, 1970; Langmuir, 1997). The common ion effect of gypsum dissolution and calcite precipitation is often accompanied by dolomite dissolution, leading to the observed increase in Mg^{2+} in groundwater. Elevated calcium concentration in group 2 waters is likely related to the ion exchange (Na^+ replacing Ca^{2+} in clays found in the area). The concentrations of Na^+ and Cl^- are relatively high away from the recharge area. The concentrations of Na^+ and Cl^- in groundwater provide evidence that halite dissolution (Triassic formation) is the major process controlling Na^+ and Cl^- in groundwater.

As group 2 water move toward central part of the plain, concentrations of major-ions increase, producing group 3 water (Table 2). The increase in major-ion concentrations of group 3 waters is a result of groundwater interactions with the basin-fill deposits and the same set of minerals used in Model 1 explains the chemistry of the group 3 water.

5. Conclusion

The results of this study showed that analysis of hydrochemical data using statistical techniques such as cluster analysis coupled with inverse geochemical modeling of the statistical clusters can help to elucidate the geologic factor controlling water chemistry. Three main chemically different water types were identified by cluster analysis based on major ion contents. Group 1 samples have a low salinity EC of 937 μS/cm. When a more effective process of water–rock interaction occurs, the waters acquire greater salinity, changing in composition towards Cl^-–HCO_3^-–Ca^{2+} (group 2) and Cl^-–Ca^{2+}–Na^+ (group 3) types. The results of saturation calculations show that all groups are super-saturated with respect to carbonate minerals. Evaporite minerals are under-saturated in all groups suggesting that their soluble component Na^+, Cl^-, Ca^{2+} and SO_4^{2-} concentrations are not limited by mineral equilibrium. The inverse geochemical modeling demonstrated that relatively few phases are required to derive water chemistry in the area. In a broad sense, the reactions responsible for the hydrochemical evolution in the area fall into three categories: (1) dissolution of evaporite minerals; (2) precipitation of carbonate minerals, quartz, kaolinite and Ca-smectite; (3) ion exchange.

References

Adams, S., Titus, R., Pietersen, K., Tredoux, G., Harris, C., 2001. Hydrochemical characteristics of aquifers near Sutherland in the western Karoo, South Africa. Journal of Hydrology 241 (1–2), 91–103.

Alberto, W.D., del Pilar, D.M., Valeria, A.M., Fabiana, P.S., Cecilia, H.A., de los Angles, B.M., 2001. Pattern recognition techniques for the evaluation of spatial and temporal variations in water quality, a case study: Suquia river basin (Cordoba–Argentina). Water Resources 35, 2881–2894.

André, L., 2002. Contribution de la géochimie à la connaissance des écoulements souterrains profonds. Application à l'aquifère des Sables Infra-Molassiques du Bassin Aquitain, Thèse: Bordeaux 3, p. 230.

APHA-AWWA-WPCF, 1995a. Standard Methods for the Examination of Water and Wastewater, 19th ed., New York, USA.

APHA, 1989. Standard Methods for Examination of Water and Wastewater, 17th ed. American Public Health Association, Washington, DC.

APHA, 1995b. Standard Methods for the Examination of Water and Wastewater, 19th ed. American public Health Association, Washington, DC.

Back, W., Hanshaw, B.B., 1970. Comparison of chemical hydrology of Florida and Yucatan. Journal of Hydrology 10, 360–368.

Belkhiri, L., Boudoukha, A., Mouni, L., Baouz, T., 2010. Application of multivariate statistical methods and inverse geochemical modeling for characterization of groundwater – a case study: Ain Azel plain (Algeria). Geoderma 159, 390–398.

Birke, M., Rauch, U., 1993. Environmental aspects of the regional geochemical survey in the southern part of east Germany. Journal of Geochemical Exploration 49 (1–2), 35–61.

Briz-Kishore, B.H., Murali, G., 1992. Factor analysis of revealing hydrochemical characteristics of a watershed. Environmental Geology and Water Sciences 19 (1), 3–9.

Cerling, T.E., Pederson, B.L., Damm, K.L.V., 1989. Sodium–calcium ion exchange in the weathering of shales: implications for global weathering budgets. Geology 17, 552–554.

Charlton, S.R., Macklin, C.L., Parkhurst, D.D., 1997. PHREEQCI – a graphical user interface for the geochemical computer program PHREEQC. US Geol. Survey Water Resources Investigation, Report (97-4222).

Chen, J., 1987. Water Environment Chemistry. Higher Education Press, Beijing, China.

Clesceri, L.S., Greenberg, A.E., Eaton, A.D., 1998. Standard Methods for the Examination of Water and Wastewater, 20th ed. American Public Health Association, American Water Works Association, Water Environment Federation, Washington.

Davis, J.C., 1986. Statistics and Data Analysis in Geology. Wiley, New York, p. 647.

Drever, J.I., 1988. The Geochemistry of Natural Waters. Prentice-Hall, New Jersey.

Eberts S.M., George L.L., 2000. Regional groundwater flow and geochemistry in the midwestern basins and Arches aquifer system in parts of Indiana, Ohio, Michigan, and IL. US Geological Survey Professional Paper 1423-C, p. 103.

Fisher, R.S., Mulican, W.F., 1997. Hydrochemical evolution of sodium-sulfate and sodium-chloride groundwater beneath the northern Chihuahuan desert, Trans-Pecos, Rexas, USA. Hydrogeology Journal 10 (4), 455–474.

Galcon, J., 1967. Recherches sur la géologie et les gîtes métallifères du Tell Sétifien, Doct Thesis Sc. Nat. Publ. Serv. Geol., from Algeria.

Garrels, R.M., Mackenzie, F.T., 1971. Evolution of Sedimentary Rocks. Norton, New York.

Guiraud, R., 1973. Evolution post-triasique de l'avant pays de la chaîne Alpine de l'Algérie, d'après l'étude du bassin d'El Eulma et les régions voisines, Thèses Sc. Nat. Nice, France.

Güler, C., Thyne, G.D., 2004. Hydrologic and geologic factors controlling surface and groundwater chemistry in Indian wells–Owens valley area, southeastern California, USA. Journal of Hydrology 285, 177–198.

Helena, B., Pardo, R., Vega, M., Barrado, E., Fernandez, J.M., Fernandez, L., 2000. Temporal evolution of ground water composition in an alluvial aquifer (Pisuerga river, Spain) by principal component analysis. Water Research 34, 807–816.

Hernandez, M.A., Gonzalez, N., Levin, M., 1991. Multivariate analysis of a coastal phreatic aquifer using hydrochemical and isotopic indicators, Buenos Aires, Argentina. In: Proceedings of the International Association on Water Pollution Research and Control's International Seminar on Pollution, Protection and Control of Ground Water, as published in Water Science & Technology, vol. 24, pp. 139–146.

Join, J.L., Coudray, J., Longworth, K., 1997. Using principal components analysis and Na/Cl ratios to trace ground water circulation in a volcanic island: the example of reunion. Journal of Hydrology 190 (1–2), 1–18.

Katz, B.G., Coplen, T.B., Bullen, T.D., Davis, J.H., 1998. Use of chemical and isotopic tracers to characterize the interaction between groundwater and surface water in mantled Karst. Groundwater 35 (6), 1014–1028.

Kuells, C., Adar, E.M., Udluft, P., 2000. Resolving patterns of ground water flow by inverse hydrochemical modeling in a semiarid Kalahari basin. Tracers and Modelling in Hydrogeology 262, 447–451.

Langmuir, D., 1997. Aqueous Environmental Geochemistry. Prentice-Hall, Upper Saddle River, NJ.

Liedholz, T., Schafmeister, M.T., 1998. Mapping of hydrochemical ground water regimes by means of multivariatestatistical analyses. In: Buccianti, A., Nardi, G., Potenza, R. (Eds.). Proceedings of the Fourth Annual Conference of the International Association for Mathematical Geology, October 5–9, Ischia, Italay, Kingston, Ontario, Canada: International Association for Mathematical Geology, pp. 298–303.

Locsey, K.L., Cox, M.E., 2003. Statistical and hydrochemical methods to compare basalt- and basement rock-hosted groundwaters: Atheron Tablelands, northeastern Australia. Environmental Geology 43 (6), 698–713.

Lopez-Chicano, M., Bouamama, M., Vallejos, A., Pulido, B.A., 2001. Factors which determine the hydrogeochemical behavior of karstic springs: a case study from the Betic Cordilleras, Spain. Applied Geochemistry 16 (9–10), 1179–1192.

Maya, A.L., Loucks, M.D., 1995. Solute and isotopic geochemistry and groundwater flow in the Central Wasatch range, Utah. Journal of Hydrology 172, 31–59.

Murray, K.S., 1996. Hydrology and geochemistry of thermal waters in the Upper Napa valley, California. Ground Water 34 (6), 1115–1124.
Ochsenkuehn, K.M., Kontoyannakos, J., Ochsenkuehn, P.M., 1997. A new approach to a hydrochemical study of groundwater flow. Journal of Hydrology 194 (1–4), 64–75.
Parkhurst, D.L., Appelo, C.A.J., 1999. User's guide to PHREEQC (ver. 2) A computer program for speciation, batch-reaction, one-dimensional transport, and inverse geochemical calculations. US Geological Survey, the Water Resources Investment, Rept (99-4259).
Pereira, H.G., Renca, S., Sataiva, J., 2003. A case study on geochemical anomaly identification through principal component analysis supplementary projection. Applied Geochemistry 18, 37–44.
Piper, A.M., 1994. A graphic procedure in geochemical interpretation of water analyses. American Geophysical Union Transactions 25, 914–923.
Plummer, L.N., Back, M., 1980. The mass balance approach: application to interpreting the chemical evolution of hydrological systems. American Journal of Science 280, 130–142.
Plummer, L.N., Sprinckle, C.L., 2001. Radiocarbon dating of dissolved inorganic carbon in groundwater from confined parts of the upper Floridan aquifer, Florida, USA. Hydrogeology Journal 9, 127–150.
Razack, M., Dazy, J., 1990. Hydrochemical characterization of groundwater mixing in sedimentary and metamorphic reservoirs with combined use of Piper's principle and factor analysis. Journal of Hydrology 114 (3–4), 371–393.
Reeve, A.S., Siegel, D.I., Glaser, P.H., 1996. Geochemical controls on peatland pore water from the Hudson bay lowland: a multivariate statistical approach. Journal of Hydrology 181 (1–4), 285–304.
Rosen, M., Jones, S., 1998. Controls of the chemical composition of groundwater from alluvial aquifers in the Wanaka and Wakatipu basins, central Otago, New Zealand. Hydrogeology Journal 6, 264–281.
Rowell, D.L., 1994. Soil Science. Methods and Applications. Longman and Scientific Technical, p. 350.
Savornin, J., 1920. Etude géologique du Hodna et du plateau Sétifien. Thèse Sc. Nat. Lyon, France.
Seyhan, E., van-de-Griend, A.A., Engelen, G.B., 1985. Multivariate analysis and interpretation of the hydrochemistry of dolomitic reef aquifer, Northern Italy. Water Resources Research 21 (7), 1010–1024.
STATISTICA® 5.0 for Windows. 1998. StatSoft, Inc., Tulsa OK. USDA, Natural Resources Conservation Services, 1999. Soil Taxonomy: A Basic System of Soil Classification for Making and Interpreting Soil Surveys. Agriculture Handbook No. 436, p. 871.
Suk, H., Lee, K.K., 1999. Characterization of a ground water hydrochemical system through multivariate analysis: clustering into ground water zones. Ground Water 37 (3), 358–366.
Swanson, S., Bahr, J., Schwar, M., Potter, K., 2001. Two-way cluster analysis of geochemical data to constrain spring source waters. Chemical Geology 179, 73–91.
Thomas, J.M., Welch, A.H., Preissler, A.M., 1989. Geochemical evolution of ground water in Smith Creek valley – a hydrologically closed basin in central Nevada, USA. Applied Geochemistry 4, 493–510.
Usunoff, E.J., Guzman-Guzman, A., 1989. Multivariate analysis in hydrochemistry: an example of the use of factor and correspondence analysis. Ground Water 27, 27–34.
Vila, J.M., 1980. La chaîne Alpine d'Algérie orientale et des confins Algéro-Tunisiens. Thesis of doctorate be-Sc. Nat. Paris VI, France.
Wang, Y., Ma, T., Luo, Z., 2001. Geostatistical and geochemical analysis of surface water leakage into ground water on a regional scale: a case study in the Liulin karst system, northwestern China. Journal of Hydrology 246 (1–4), 223–234.
WHO, 2006. Guidelines for Drinking-Water Quality, third ed., vol. 1 – Recommendations. Word Health Organization, Geneva.
Zhu, C., Anderson, G., 2002. Environmental Application of Geochemical Modeling. Cambridge University Press, Cambridge.